

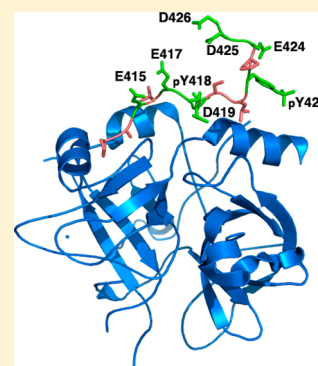
# Role of Electrostatic Interactions in Binding of Thrombin to the Fibrinogen $\gamma'$ Chain

Kristine S. Alexander,<sup>†</sup> Michael G. Fried,<sup>§</sup> and David H. Farrell<sup>\*,‡</sup>

<sup>†</sup>Department of Molecular and Medical Genetics and <sup>‡</sup>Department of Medicine, Oregon Health & Science University, Portland, Oregon 97239-3098, United States

<sup>§</sup>Department of Biochemistry and Molecular Biology, University of Kentucky, Lexington, Kentucky 40536-0001, United States

**ABSTRACT:** Thrombin binds to the highly anionic fibrinogen  $\gamma'$  chain through anion-binding exosite II. This binding profoundly alters thrombin's ability to cleave substrates, including fibrinogen, factor VIII, and PAR1. However, it is unknown whether this interaction is due mainly to general electrostatic complementarity between the  $\gamma'$  chain and exosite II or if there are critical charged  $\gamma'$  chain residues involved. We therefore systematically determined the contribution of negatively charged amino acids in the  $\gamma'$  chain, both individually and collectively, to thrombin binding affinity. Surface plasmon resonance binding experiments were performed using immobilized  $\gamma'$  chain peptides with charged-to-uncharged amino acid substitutions, i.e., Asp to Asn, Glu to Gln, and pTyr to Tyr. Individually, the substitution of uncharged for charged amino acids resulted in only minor changes in binding affinity, with a maximal change in  $K_d$  from 0.440 to 0.705  $\mu$ M for the Asp419Asn substitution. However, substitution of all three charged amino acids in a conserved  $\beta$ -turn that is predicted to contact thrombin, pTyr418Tyr, Asp419Asn, and pTyr422Tyr, resulted in the loss of measurable binding, as did substitution of all the flanking charged amino acids. In addition, the binding of the  $\gamma'$  chain to thrombin was weakened in a dose-dependent manner with increasing NaCl concentration, resulting in a net loss of three or four ion pairs between thrombin and the  $\gamma'$  chain. Therefore, although each of the individual charges in the  $\gamma'$  chain contributes only incrementally to the overall binding affinity, the ensemble of the combined charges plays a profound role in the thrombin– $\gamma'$  chain interactions.



Thrombin, a trypsin-like serine protease, plays a central role in blood coagulation.<sup>1</sup> Thrombin cleavage is responsible for activating several of the coagulation factors, including fibrinogen, which is then converted to the insoluble fibrin fibers that make up the protein meshwork of the blood clot. On its surface, adjacent to its active site, thrombin contains two basic regions, exosites I and II. These anion-binding exosites function to modulate thrombin's activity and specificity.<sup>2–5</sup> Their proximity to the active site allows for direct involvement in the recognition of thrombin substrates, and cofactors and anticoagulant drugs utilize these exosites to alter thrombin–substrate interactions. Fibrin(ogen) contains two sites that interact with these thrombin exosites: a low-affinity site in the fibrinogen central E domain and a higher-affinity site in the carboxy terminus of the  $\gamma'$  fibrinogen variant.<sup>6</sup>

Fibrinogen is a dimeric molecule, containing two each of three types of polypeptide chains:  $A\alpha$ ,  $B\beta$ , and  $\gamma$ . The  $\gamma'$  fibrinogen isoform contains a  $\gamma'$  chain, produced through alternative splicing of the  $\gamma$  chain mRNA.<sup>7,8</sup> The  $\gamma'$  chain differs from the more abundant  $\gamma A$  at the carboxy terminus, where it has 20 residues (<sup>408</sup>VRPEHPAETE<sub>s</sub>YDSL<sub>s</sub>YPEDDL<sup>427</sup>) in place of the last four residues (<sup>408</sup>AGDV<sup>411</sup>) of the  $\gamma A$  chain. This extended C-terminus provides  $\gamma'$  fibrinogen with unique biochemical properties compared to those of the more common isoform, particularly the high-affinity binding site for thrombin,<sup>9</sup> and studies suggest that the  $\gamma'$  fibrinogen may also serve as a carrier for factor XIII.<sup>10,11</sup>

Competitive binding experiments have demonstrated that  $\gamma'$  fibrinogen binds to thrombin anion-binding exosite II, the same region that binds to heparin.<sup>12</sup> One hypothesis is that  $\gamma'$  fibrin may function to retain thrombin at the site of the clot, as fibrin-bound thrombin remains active<sup>13</sup> and thrombin dissociates more slowly from clots containing  $\gamma'$  fibrin than from clots made with  $\gamma A$  fibrin alone.<sup>14</sup> Additionally, clot-bound thrombin is resistant to inhibition by antithrombin.<sup>14</sup> There is also evidence that binding to the  $\gamma'$  fibrin(ogen) carboxy terminus inhibits thrombin's cleavage of factor VIII, alters fibrin clot formation,<sup>15</sup> and inhibits thrombin cleavage of platelet PAR1.<sup>16,17</sup>

A number of studies have investigated the interaction between thrombin and  $\gamma'$  fibrinogen using  $\gamma'$  carboxy-terminal peptides. The  $\gamma'$  carboxy terminus is highly anionic, containing four glutamic acid residues, three aspartic acid residues, and two sulfotyrosine residues,<sup>18,19</sup> while the corresponding binding site on thrombin, exosite II, is highly positively charged. It is therefore expected that the binding of the  $\gamma'$  410–427 peptide to thrombin is at least partially due to this electrostatic complementarity. This cannot be the entire basis for the interaction, however, as experiments using a reversed sequence of the 414–427 peptide demonstrated greatly reduced affinity.<sup>9</sup>

Received: November 1, 2011

Revised: March 21, 2012

Published: March 22, 2012



Table 1. Binding Affinities of the Charged-to-Uncharged  $\gamma'$  Peptides<sup>a</sup>

Peptide	Sequence	$K_d$ ( $\mu$ M) (mean $\pm$ standard error of the mean)	$P$ value (compared to wild-type)*
Wild-type	PEHPAETE <sub>p</sub> YDSL <sub>p</sub> YPEDDL	0.440 $\pm$ 0.011	—
#1	PQHPAETE <sub>p</sub> YDSL <sub>p</sub> YPEDDL	0.441 $\pm$ 0.016	1.00
#2	PEHPAQTE <sub>p</sub> YDSL <sub>p</sub> YPEDDL	0.485 $\pm$ 0.011	0.46
#3	PEHPAQTE <sub>p</sub> YDSL <sub>p</sub> YPEDDL	0.541 $\pm$ 0.010	0.025
#4	PEHPAETE <sub>p</sub> YDSL <sub>p</sub> YPEDDL	0.583 $\pm$ 0.011	0.008
#5	PEHPAETE <sub>p</sub> YNSL <sub>p</sub> YPEDDL	0.705 $\pm$ 0.011	<0.001
#6	PEHPAETE <sub>p</sub> YDSL <sub>p</sub> YPEDDL	0.702 $\pm$ 0.021	0.018
#7	PEHPAETE <sub>p</sub> YDSL <sub>p</sub> YPQDDL	0.582 $\pm$ 0.018	0.073
#8	PEHPAETE <sub>p</sub> YDSL <sub>p</sub> YPENDL	0.608 $\pm$ 0.019	0.053
#9	PEHPAETE <sub>p</sub> YDSL <sub>p</sub> YPEDNL	0.465 $\pm$ 0.010	1.00
#10	PEHPAETE <sub>p</sub> YNSL <sub>p</sub> YPEDDL	—	—
#11	PQHPAQTE <sub>p</sub> YDSL <sub>p</sub> YPQNNL	—	—
#12	PQHPAQTE <sub>p</sub> YDSL <sub>p</sub> YPEDDL	1.968 $\pm$ 0.025	<0.001
#13	PEHPAETE <sub>p</sub> YDSL <sub>p</sub> YPQNNL	3.189 $\pm$ 0.034	0.002

<sup>a</sup>BIAevaluation was used to calculate affinity constants ( $K_d$ ) based on a 1:1 Langmuir binding model. The standard error of the mean was calculated from triplicate determinations. \* $P$  values were adjusted for multiple comparisons using Bonferroni correction.

Studies using deleted peptides have indicated that residues 411–427 are involved in this binding and that further truncation at the amino or carboxy terminus significantly weakens or abrogates the interaction.<sup>9,12</sup> Sulfation<sup>9</sup> or phosphorylation<sup>12,20</sup> of the peptide's two tyrosine residues also appears to be necessary for maximal binding, with a considerable decrease in affinity for peptides with only a single modified tyrosine. There is evidence that the negative charge of Tyr422 may be more important than that of Tyr418.<sup>9,20</sup>

The crystal structure of the thrombin– $\gamma'$  peptide complex determined by Pineda et al.<sup>21</sup> confirms many of the findings from other studies. The structure showed that the interaction of the  $\gamma'$  peptide with thrombin was similar to that of heparin, with numerous electrostatic interactions between the cationic residues of exosite II and the anionic residues of the  $\gamma'$  peptide. The peptide's phosphotyrosines are closely associated with positively charged residues in exosite II, with pTyr418 interacting with Arg126, Lys235, and Lys236, and pTyr422 with Lys240. Interestingly, this structure shows the peptide in contact with two thrombin molecules, but the significance of this finding is uncertain and may represent a crystal packing artifact.

While the crystal structure and other studies have implicated regions of the peptide important for thrombin binding, the individual contribution of each of the peptide's charged residues to this binding has not been determined. In this paper, we test the predictions of the crystal structure by examining these contributions systematically, using peptides with charged-to-uncharged substitutions, and measuring the thrombin binding affinities using surface plasmon resonance. These experiments are designed to determine whether the  $\gamma'$  chain–thrombin interaction is due mainly to cooperative binding of the ensemble of charge residues or if there are critical charged residues in the peptide that are required for binding.

## EXPERIMENTAL PROCEDURES

**Materials.** N-Terminally biotinylated  $\gamma'$  peptide was synthesized by Abgent (San Diego, CA). N-Terminally biotinylated analogue peptides were synthesized by Abgent and Anaspec (Fremont, CA). See Table 1 for peptide sequences. All peptides were >95% pure, with the peptide purity verified by high-performance liquid chromatography and mass spectrometry. FPRck-inhibited thrombin was purchased from Enzyme Research Laboratories (South Bend, IN). Series S Sensor Chips SA and HBS-EP+ [10 mM HEPES (pH 7.4), 150

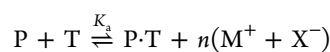
mM NaCl, 0.05% P20 surfactant, and 3 mM EDTA] buffer were purchased from GE Healthcare Biosciences Corp. (Piscataway, NJ).

**Surface Plasmon Resonance.** Surface plasmon resonance experiments were performed with a Biacore T100 instrument (GE Healthcare). Biotinylated peptides were immobilized on streptavidin chips following the manufacturer's instructions. Briefly, flow cell surfaces were prepared for immobilization with three 60 s injections of 1 M NaCl and 50 mM NaOH. Biotinylated peptides were immobilized to sensor chip flow cells at a level of 150 response units (RU). Reference flow cells without immobilized peptide were used as controls.

All peptide–thrombin binding assays were performed at 25 °C. HBS-EP+ was used as both running and binding buffer. Various concentrations of FPRck–thrombin were injected over flow cells bound with wild-type and analogue peptides until equilibrium binding was reached. Kinetic injections were performed for 20 s at a flow rate of 50  $\mu$ L/min, followed by a 30 s dissociation time. No regeneration of the flow cells following injections was necessary. Buffer-only injections were included for each condition, and these responses were subtracted from the binding signals. Responses from control flow cells were similarly subtracted to account for changes in the refractive index. BIAevaluation was used to calculate affinity constants ( $K_d$ ) based on a 1:1 Langmuir binding model.  $K_d$  determinations for each analogue peptide were based on three replicate experiments using freshly prepared thrombin dilutions.

For experiments with NaCl concentrations of 200–350 mM, calculated  $K_d$  values were greater than the highest concentration of thrombin used. Because the equilibrium affinity analysis calculates  $K_d$  as the concentration of analyte at which half-maximal binding occurs,  $K_d$  values outside the range of analyte concentrations used cannot be accurately determined. To address this problem, the maximal binding response for the flow cells used for these experiments was measured in binding experiments with buffer containing 150 mM NaCl, and this value was used to correct the calculated  $K_d$  for the higher-salt experiments.

The salt concentration-dependent peptide–thrombin interaction can be written as



where  $P$  and  $T$  represent peptide and thrombin (with associated counterions), respectively,  $P \cdot T$  is the peptide–

thrombin complex (with associated counterions),<sup>22</sup>  $M^+$  and  $X^-$  are cations and anions bound or released on complex formation, and  $n$  is the net ion stoichiometry (net ion release is indicated by  $n > 0$ ; net ion uptake is indicated by  $n < 0$ ). The equilibrium association constant is given by

$$K_a = \frac{[P \cdot T][MX]^n}{[P][T]}$$

Thus, a graph of  $\ln K_{obs}$  as a function of  $\ln [MX]$  should have a slope of  $-n$ .

## RESULTS

**Kinetics of Binding of Thrombin to the  $\gamma'$  Peptide.** To test the contributions of the individual charged residues in the  $\gamma'$  carboxy-terminal peptide to thrombin binding, we performed binding studies using the wild-type peptide as well as analogue peptides in which negatively charged residues were replaced individually with uncharged residues with a similar side chain size, Glu-to-Gln, Asp-to-Asn, and pTyr-to-Tyr (see Table 1 for peptide sequences). Figure 1 shows the locations of the

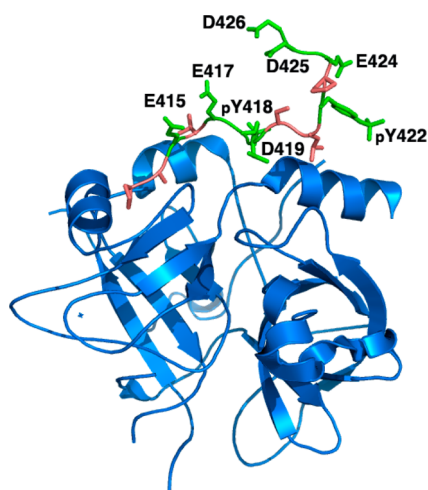


**Figure 1.** Crystal structure of thrombin in complex with the  $\gamma'$  peptide. Residues substituted in our experiments are colored green. Note that the structure does not predict the positions of the N-terminal residues Pro410–His412; these residues, including the Glu411 altered in peptide 1, are not shown.

negatively charged residues of the  $\gamma'$  peptide in complex with thrombin according to the crystal structure of Pineda et al.<sup>21</sup>

Interactions between these peptides and thrombin were studied by surface plasmon resonance (SPR) using a Biacore T100 instrument. The peptides were immobilized to a chip surface, and solutions containing thrombin were passed over the chip until equilibrium binding was achieved. The kinetics of binding demonstrated a rapid  $k_{on}$  rate as well as a rapid  $k_{off}$  rate, resulting in square wave-like binding isotherms (Figure 2). Kinetic quantitation of these interactions was not possible, as both the association and dissociation were extremely rapid and, in the case of the dissociation rate, outside the limits of quantification for the instrument. For this reason, equilibrium affinity analyses were performed to measure the  $K_d$  for the binding interaction.

The wild-type  $\gamma'$  peptide bound thrombin with a  $K_d$  ( $\pm$ standard error) of  $0.440 \pm 0.011 \mu\text{mol/L}$ , which is similar to the affinity of  $0.63 \mu\text{mol/L}$  found previously by fluorescence polarization<sup>12</sup> and the  $K_d$  of  $0.20 \mu\text{mol/L}$  measured for the

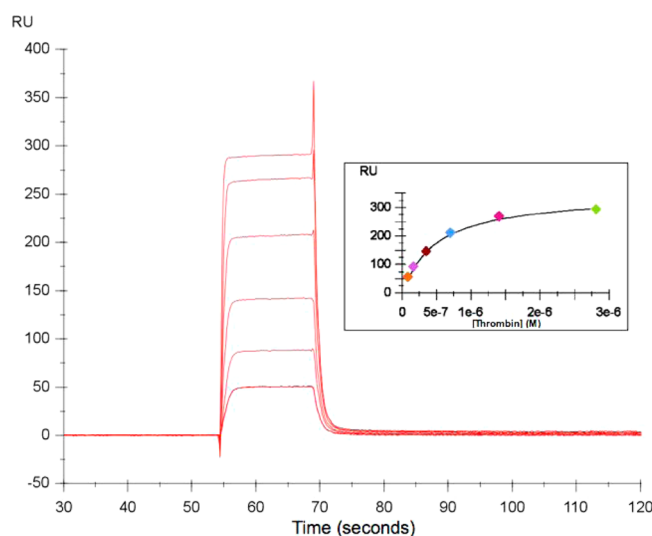


**Figure 2.** Binding isotherms for binding of thrombin to the immobilized wild-type  $\gamma'$  peptide using surface plasmon resonance. Increasing concentrations of thrombin were bound to the wild-type  $\gamma'$  peptide in a Biacore instrument at 25 °C until equilibrium binding was reached, and the resonance units were quantitated with time. Kinetic injections were performed for 20 s, followed by a 30 s dissociation time. The inset shows the maximal binding as measured in resonance units as a function of thrombin concentration. BIAevaluation was used to calculate affinity constants ( $K_d$ ) based on a 1:1 Langmuir binding model.

binding of thrombin to  $\gamma'$  fibrinogen.<sup>9</sup> The rapid  $k_{on}$  and  $k_{off}$  rates are apparent in the binding isotherms for these experiments (Figure 2).

**Binding of Thrombin to Analogue  $\gamma'$  Peptides.** The single-residue charged-to-uncharged analogue peptides bound thrombin with affinities ranging from  $0.441$  to  $0.705 \mu\text{mol/L}$  (Table 1). The analogue peptides with substitutions in the first two or last four charged residues (peptides 1, 2, and 7–9) did not differ from the wild-type peptide with respect to thrombin affinity, while the other analogue peptides exhibited significantly lower affinities. In particular, peptides 5 and 6, corresponding to changes of Asp419Asn and pTyr422Tyr, respectively, bound thrombin with the lowest affinities. These residues have been shown by two-dimensional nuclear magnetic resonance (NMR) to assume a  $\beta$ -turn conformation<sup>20</sup> and contact thrombin exosite II.<sup>21</sup>

Sulfation (or phosphorylation) of the  $\gamma'$  peptide's two Tyr residues has been shown to be important for thrombin binding,<sup>9,12</sup> and our results confirm and extend these findings, with a significant decrease in affinity seen with either monophosphorylated peptides, pTyr418Tyr and pTyr422Tyr. We found that removal of the negative charge on Tyr422 reduced the thrombin affinity more than removal of the Tyr418 charge, in agreement with other reports.<sup>9,20</sup>

In addition to pTyr418 and pTyr422, the Pineda crystal structure<sup>21</sup> predicts a number of contacts between thrombin exosite II and Asp419 of the  $\gamma'$  peptide, located between the phosphotyrosines. These three residues, along with Glu415, are the only charged residues predicted to interact with exosite II on a single thrombin molecule. This is an important feature of the crystal structure model, because the cocrystal depicts two thrombin molecules bound to a single  $\gamma'$  chain.<sup>21</sup> We therefore sought to determine whether these three residues were required for thrombin interaction, and if they were able to mediate this

binding in the absence of the other anionic residues. SPR studies using a peptide with uncharged replacements pTyr418Tyr, Asp419Asn, and pTyr422Tyr (peptide 10) demonstrated a complete absence of measurable binding (Figure 3). Conversely, experiments with a peptide in which

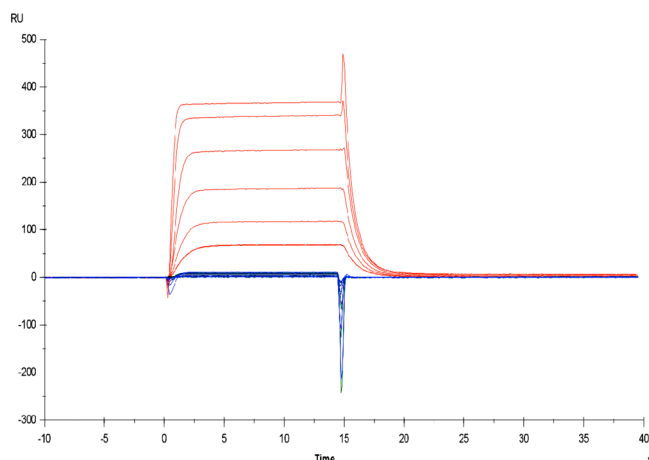


**Figure 3.** Thrombin binding curves for the wild-type  $\gamma'$  peptide (red) and analogue peptides 10 and 11 (blue and green, respectively). The data show that neither peptide 10 with the central three charged-to-uncharged amino acid changes (pTyr418Tyr, Asp419Asn, and pTyr422Tyr) nor peptide #11 with flanking charged-to-uncharged amino acid changes (Glu411Gln, Glu415Gln, Glu417Gln, Glu424Gln, Asp425Asn, and Asp426Asn) displayed measurable binding.

all other negatively charged residues were substituted instead (peptide 11) also showed no measurable interaction with thrombin (Figure 3), indicating that these three charged residues, while necessary for thrombin binding, are not sufficient in the absence of the other negatively charged residues. To further investigate this, we performed binding experiments using peptides that had either the amino-terminal three charges (peptide 12) or the carboxyl-terminal three charges (peptide 13) substituted with uncharged residues. These peptides demonstrated substantially reduced binding affinities as compared with those of the singly substituted peptides, but unlike peptide 10, did have measurable binding.

**Effect of NaCl Concentration on Thrombin– $\gamma'$  Peptide Affinity.** To further investigate the nature of thrombin– $\gamma'$  peptide interactions, we determined the dependency of the binding on ionic strength. Binding studies were performed in the presence of increasing concentrations of salt at 150, 200, 250, and 350 mM NaCl (Table 2). These experiments demonstrated a strong salt dependence of the binding, with an increase in NaCl concentration from 150 to 200 mM associated with a 12-fold decrease in affinity, from 0.488 to 6.05  $\mu\text{mol/L}$ , respectively. Increasing the NaCl concentration to 250 mM resulted in an additional 3.1-fold decrease in affinity to 18.6  $\mu\text{mol/L}$ . Further increasing the salt concentration to 350

**Table 2. Dependence of Thrombin– $\gamma'$  Peptide Binding on NaCl Concentration**

[NaCl] (mM)	$K_d$ ( $\mu\text{M}$ ) (mean $\pm$ standard error of the mean)
150	$0.488 \pm 0.042$
200	$6.05 \pm 0.64$
250	$18.6 \pm 0.98$
300	$120 \pm 2.1$

mM resulted in an additional 6.5-fold decrease in affinity to 120  $\mu\text{mol/L}$ , a greater than 240-fold decrease in affinity compared to that of normal saline. These results demonstrate a significant electrostatic component to the thrombin– $\gamma'$  peptide interaction.

To quantitate the release of counterions during the binding of thrombin to the  $\gamma'$  peptide, the dependence of the natural logarithm of the  $K_a$  on the natural logarithm of the NaCl concentration was investigated (Figure 4). The slope indicates

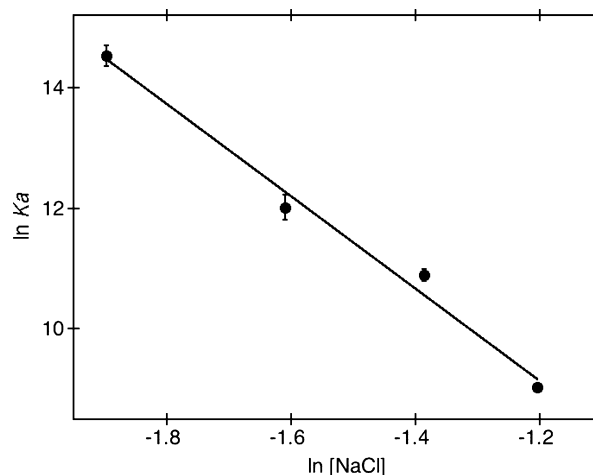


**Figure 4.** Linkage plot. The slope indicates a net release of  $7.6 \pm 0.6$  ions for the binding of thrombin to the  $\gamma'$  peptide. Assuming that counterions are released from protein groups forming ion pairs, the data indicate that three or four ion pairs formed between thrombin and the  $\gamma'$  peptide, with net release to solvent of associated counterions.

that there was a net release of  $7.6 \pm 0.6$  ions in the binding reaction. Assuming a 1:1 stoichiometry, there may be three or four ion pairs formed between the  $\gamma'$  peptide and thrombin, with net release to solvent of the associated counterions.

## DISCUSSION

It has been shown previously that the highly anionic carboxy terminus of the  $\gamma'$  fibrinogen chain binds to exosite II of thrombin<sup>12</sup> and modulates the activity of thrombin toward several of its substrates.<sup>14–17</sup> The crystal structure of thrombin in complex with the  $\gamma'$  carboxy-terminal peptide, along with binding studies, has implicated several residues and regions of the peptide as being important for this binding. In this work, we have further examined the binding contributions made by each of the peptide's negatively charged residues and investigated the salt dependence of this interaction using SPR.

The  $k_{\text{on}}$  and  $k_{\text{off}}$  rates for the binding of thrombin to the  $\gamma'$  peptide were quite rapid. It is tempting to speculate that such rapid binding may serve to increase the local thrombin concentration surrounding the growing fibrin clot in the presence of rapidly flowing blood. A similar strategy is employed in the catch bonds between platelet glycoprotein Ib and von Willebrand factor and allows rapidly moving platelets to be slowed by sequential tethering events to von Willebrand factor coated on injured subendothelium.<sup>23</sup> The  $\gamma'$  chain–thrombin exosite II interaction by itself would result in both a rapid association and a rapid dissociation. However, during blood coagulation, thrombin also interacts with intact fibrin through exosite I.<sup>24</sup> The additional interaction between exosite



I and fibrin may further stabilize the initial complex between exosite II and the  $\gamma'$  chain. Thrombin has been visualized on the growing clot surface using intravital microscopy,<sup>25</sup> although the cognate receptor for thrombin on the clot remains unclear. Thrombin bound to fibrin is also protected from inactivation by antithrombin.<sup>14</sup>

Altering the charged residues in the  $\gamma'$  chain had differential effects on thrombin binding, depending upon their location. Substituting many of the charged residues, including Gln411 for Glu, appeared to have no effect, although several previous studies have indicated that amino-terminal truncation of the peptide from Pro410 or Glu411 to Ala414 results in a significant decrease in affinity.<sup>9,12,20</sup> However, the reduced affinity seen with the truncated peptides likely has less to do with the loss of the charge on Glu411 and more to do with other interactions of the side chain with thrombin. This hypothesis is supported both by our results and by the Pineda crystal structure, which predicts interactions between Pro413 of the peptide and Val163 and Arg165 of thrombin,<sup>21</sup> as well as NMR data by Sabo et al. that indicate a lack of contact between thrombin and residues Pro410–His412.<sup>20</sup>

Both the crystal structure and the NMR study by Sabo et al. predict a  $\beta$ -turn conformation in the region that includes Tyr422 and Asp425.<sup>20,21</sup> In the crystal structure, this  $\beta$ -turn bridges exosite II of a second, symmetry-related thrombin molecule and predicts interactions between the peptide's Asp426 and Arg93 on thrombin. In our experiments, the replacement of Asp426 on the  $\gamma'$  peptide had no effect on thrombin binding. Many of the charged  $\gamma'$  peptide residues that are implicated in thrombin binding in the crystal structure<sup>21</sup> appeared to influence binding affinity in our study. These include pTyr418, Asp419, and pTyr422. These data tend to support the Pineda model of two thrombin molecules binding to a single  $\gamma'$  chain, although the lack of an effect of the Asp426Asn substitution on binding affinity is puzzling. The structure also did not contain electron density for residues 410–412, which, along with our data showing that Glu411 does not contribute to binding and the results of N-terminal deletion studies, indicates that this region does not have any important interactions with exosite II.

Taken together, these results demonstrate the significant role of electrostatic interactions between thrombin anion-binding exosite II and the fibrinogen  $\gamma'$  chain. However, while each of the individual charges contributes only incrementally to the overall binding affinity, the ensemble of the combined charges plays a profound role in the thrombin– $\gamma'$  chain interactions.

## AUTHOR INFORMATION

### Corresponding Author

\*Phone: (503) 494-8602. Fax: (503) 222-2306. E-mail: farrell@ohsu.edu.

### Funding

This work was supported by National Institutes of Health Grant HL097298.

### Notes

The authors declare the following competing financial interest(s): Oregon Health & Sciences University (OHSU) and Dr. David Farrell have a significant interest in Gamma Therapeutics, a company that may have a commercial interest in the results of this research and technology. This potential individual and institutional conflict of interest has been reviewed and managed by OHSU.

## ACKNOWLEDGMENTS

We thank Dr. José López of the Puget Sound Blood Center for the use of the Biacore instrument and Dr. Jason Schuman of GE Healthcare for advice on the interpretation of the Biacore data.

## REFERENCES

- (1) Di Cera, E. (2008) Thrombin. *Mol. Aspects Med.* 29, 203–254.
- (2) Ng, N. M., Quinsey, N. S., Matthews, A. Y., Kaiserman, D., Wijeyewickrema, L. C., Bird, P. I., Thompson, P. E., and Pike, R. N. (2009) The effects of exosite occupancy on the substrate specificity of thrombin. *Arch. Biochem. Biophys.* 489, 48–54.
- (3) Nimjee, S. M., Oney, S., Volovyk, Z., Bompiani, K. M., Long, S. B., Hoffman, M., and Sullenger, B. A. (2009) Synergistic effect of aptamers that inhibit exosites 1 and 2 on thrombin. *RNA* 15, 2105–2111.
- (4) Yang, L., Manithody, C., Qureshi, S. H., and Rezaie, A. R. (2010) Contribution of exosite occupancy by heparin to the regulation of coagulation proteases by antithrombin. *Thromb. Haemostasis* 103, 277–283.
- (5) Zarpellon, A., Celikel, R., Roberts, J. R., McClintock, R. A., Mendolicchio, G. L., Moore, K. L., Jing, H., Varughese, K. I., and Ruggeri, Z. M. (2011) Binding of  $\alpha$ -thrombin to surface-anchored platelet glycoprotein Iba sulfotyrosines through a two-site mechanism involving exosite I. *Proc. Natl. Acad. Sci. U.S.A.* 108, 8628–8633.
- (6) Meh, D. A., Siebenlist, K. R., and Mosesson, M. W. (1996) Identification and characterization of the thrombin binding sites on fibrin. *J. Biol. Chem.* 271, 23121–23125.
- (7) Chung, D. W., and Davie, E. W. (1984)  $\gamma$  and  $\gamma'$  chains of human fibrinogen are produced by alternative mRNA processing. *Biochemistry* 23, 4232–4236.
- (8) Fornace, A. J., Jr., Cummings, D. E., Comeau, C. M., Kant, J. A., and Crabtree, G. R. (1984) Structure of the human  $\gamma$ -fibrinogen gene. Alternate mRNA splicing near the 3' end of the gene produces  $\gamma$ A and  $\gamma$ B forms of  $\gamma$ -fibrinogen. *J. Biol. Chem.* 259, 12826–12830.
- (9) Meh, D. A., Siebenlist, K. R., Brennan, S. O., Holyst, T., and Mosesson, M. W. (2001) The amino acid sequence in fibrin responsible for high affinity thrombin binding. *Thromb. Haemostasis* 85, 470–474.
- (10) Siebenlist, K. R., Meh, D. A., and Mosesson, M. W. (1996) Plasma factor XIII binds specifically to fibrinogen molecules containing  $\gamma'$  chains. *Biochemistry* 35, 10448–10453.
- (11) Moaddel, M., Farrell, D. H., Daugherty, M. A., and Fried, M. G. (2000) Interactions of human fibrinogens with factor XIII: Roles of calcium and the  $\gamma'$  peptide. *Biochemistry* 39, 6698–6705.
- (12) Lovely, R. S., Moaddel, M., and Farrell, D. H. (2003) Fibrinogen  $\gamma'$  chain binds thrombin exosite II. *J. Thromb. Haemostasis* 1, 124–131.
- (13) Pospisil, C. H., Stafford, A. R., Fredenburgh, J. C., and Weitz, J. I. (2003) Evidence that both exosites on thrombin participate in its high affinity interaction with fibrin. *J. Biol. Chem.* 278, 21584–21591.
- (14) Fredenburgh, J. C., Stafford, A. R., Leslie, B. A., and Weitz, J. I. (2008) Bivalent binding to  $\gamma$ A/ $\gamma'$ -fibrin engages both exosites of thrombin and protects it from inhibition by the antithrombin-heparin complex. *J. Biol. Chem.* 283, 2470–2477.
- (15) Lovely, R. S., Boshkov, L. K., Marzec, U. M., Hanson, S. R., and Farrell, D. H. (2007) Fibrinogen  $\gamma'$  chain carboxy terminal peptide selectively inhibits the intrinsic coagulation pathway. *Br. J. Haematol.* 139, 494–503.
- (16) Lancellotti, S., Rutella, S., De Filippis, V., Pozzi, N., Rocca, B., and De Cristofaro, R. (2008) Fibrinogen-elongated  $\gamma$  chain inhibits thrombin-induced platelet response, hindering the interaction with different receptors. *J. Biol. Chem.* 283, 30193–30204.
- (17) Lovely, R. S., Rein, C. M., White, T. C., Jouihan, S. A., Boshkov, L. K., Bakke, A. C., McCarty, O. J., and Farrell, D. H. (2008)  $\gamma$ A/ $\gamma'$  fibrinogen inhibits thrombin-induced platelet aggregation. *Thromb. Haemostasis* 100, 837–846.

- (18) Farrell, D. H., Mulvihill, E. R., Huang, S. M., Chung, D. W., and Davie, E. W. (1991) Recombinant human fibrinogen and sulfation of the  $\gamma'$  chain. *Biochemistry* 30, 9414–9420.
- (19) Henschen, A. H. (1993) Human fibrinogen-structural variants and functional sites. *Thromb. Haemostasis* 70, 42–47.
- (20) Sabo, T. M., Farrell, D. H., and Maurer, M. C. (2006) Conformational analysis of  $\gamma'$  peptide (410–427) interactions with thrombin anion binding exosite II. *Biochemistry* 45, 7434–7445.
- (21) Pineda, A. O., Chen, Z. W., Marino, F., Mathews, F. S., Mosesson, M. W., and Di Cera, E. (2007) Crystal structure of thrombin in complex with fibrinogen  $\gamma'$  peptide. *Biophys. Chem.* 125, 556–559.
- (22) Cantor, C. R., and Schimmel, P. R. (1980) The behavior of biological molecules. In *Biophysical Chemistry Part III*, pp 871–873, W. H. Freeman and Co., San Francisco.
- (23) Interlandi, G., and Thomas, W. (2010) The catch bond mechanism between von Willebrand factor and platelet surface receptors investigated by molecular dynamics simulations. *Proteins* 78, 2506–2522.
- (24) Kaczmarek, E., and McDonagh, J. (1988) Thrombin binding to the  $A\alpha$ -,  $B\beta$ -, and  $\gamma$ -chains of fibrinogen and to their remnants contained in fragment E. *J. Biol. Chem.* 263, 13896–13900.
- (25) Bellido-Martin, L., Chen, V., Jasuja, R., Furie, B., and Furie, B. C. (2011) Imaging fibrin formation and platelet and endothelial cell activation *in vivo*. *Thromb. Haemostasis* 105, 776–782.